follows the same trend as those of the σ components. However this simple description does not explain the magnitude of the couplings in the Tempo adducts, **6** and **7**, compared to those observed in the nitronyl analogues. Fortunately, however, in compounds **1** and **7**, the Rh-O(nitroxyl) distances and the structural characteristics of the dirhodium fragments are almost identical; thus a quantitative comparison was attempted.

The magnetic orbitals are defined as singly occupied orbitals centered on the nitroxyl groups, A and B, respectively, and partially delocalized on the dirhodium fragment. Taking into account that the two compounds are centrosymmetric, these orbitals may be written at the first order of perturbation theory as

$$\Phi A = a\mathrm{Rh}(\sigma) + \mathrm{NOA}(\pi^*)$$

$$\Phi B = a\mathrm{Rh}(\sigma) + \mathrm{NOB}(\pi^*)$$

where $a = \langle \mathrm{NO}(\pi^*)||H||\mathrm{Rh}(\sigma)\rangle/\Delta$, H being the monoelectronic Hamiltonian, $\mathrm{NOA}(\pi^*)$ and $\mathrm{NOB}(\pi^*)$ the SOMO's of the two nitroxides, $\mathrm{Rh}(\sigma)$ the matching dirhodium MO, and Δ the energy gap between the NO and the Rh orbitals. The antiferromagnetic interaction is proportional to $-S^2$, with

$$S = \langle \Phi A/\Phi B\rangle = a^2\langle \mathrm{Rh}(\sigma)/\mathrm{Rh}(\sigma)\rangle + 2a\langle \mathrm{Rh}(\sigma)/\mathrm{NO}(\pi^*)\rangle + \langle \mathrm{NOA}(\pi^*)/\mathrm{NOB}(\pi^*)\rangle$$

Since the unpaired electrons are expected to be mainly localized on the nitroxides, a is small, and $a^2\langle \mathrm{Rh}(\sigma)/\mathrm{Rh}(\sigma)\rangle$ can be neglected. In addition, direct $\langle \mathrm{NO}/\mathrm{NO}\rangle$ overlap is expected to be very weak because no internitroxyl coupling would be observed if the rhodium fragment was absent; therefore, $\langle \mathrm{NO}(\pi^*)/\mathrm{NO}(\pi^*)\rangle$ can also be neglected. Thus,

$$\begin{aligned} S &\approx 2a\langle \mathrm{Rh}(\sigma)/\mathrm{NO}(\pi^*)\rangle \\ &\approx 2\langle \mathrm{Rh}(\sigma)/H/\mathrm{NO}(\pi^*)\rangle\langle \mathrm{Rh}(\sigma)/\mathrm{NO}(\pi^*)\rangle/\Delta \\ &\approx 2\langle \mathrm{Rh}(\sigma)/\mathrm{NO}(\pi^*)\rangle^2/\Delta \end{aligned}$$

The π^* nitroxyl orbitals are linear combinations of the form

$$\mathrm{NO}(\pi^*) = c2\mathrm{p(O)} + d2\mathrm{p(N)} + \ldots$$

in which only the 2p orbital of the bound oxygen atom (2p(O)) is expected to contribute significantly to the magnetic orbitals. Thus

$$S \approx 2c^2\langle \mathrm{Rh}(\sigma)/2\mathrm{p(O)}\rangle^2 = 2\rho\langle \mathrm{Rh}(\sigma)/2\mathrm{p(O)}\rangle^2$$

where ρ is the spin population on the bound oxygen atom (Table VIII). Assuming that the energy gap between the interacting orbitals is the same in compounds **1** and **7** and taking the values of the overlap integrals as $\sin\delta \sin\tau$ from Table X, one obtains

$$(S_1/S_7)^2 = \{(\rho_1/\rho_7)(\sin\delta_1 \sin\tau_1/\sin\delta_7 \sin\tau_7)\}^2$$

$$= (0.16/0.31)^2*(0.84/0.71)^2 = 0.36$$

This value is in fairly good agreement with the experimental ratio

$$J_1/J_7 = 167/538 = 0.31$$

It appears therefore, that a σ mechanism explains quantitatively the magnetic data for the two closely related complexes **1** and **7**.

Thus, an appropriate view of the bonding in these adducts implies that a σ or σ^* orbital of the metal fragment is close in energy with the π^* nitroxyl orbitals. A qualitative support to this view comes from EHT calculations performed on compound **1** and on the fragments (the nitronyl nitroxide and the metal fragment), using the structural results. The magnetic orbitals, Φ_A and Φ_B are found at -11.67 ev, each resulting from an interaction of the SOMO of one nitroxide with both the σ (-13.14 ev) and the σ^* (-11.31 ev) orbitals of the dirhodium fragment. In addition, there is a weak contribution of the π^* orbitals of the metal fragment lying at -12.07 ev. Therefore, these calculations show that the interaction between the SOMO's of the two nitroxides and the rhodium dimer moiety involves mainly the metal orbitals of σ symmetry. This result is in complete agreement with the experimental conclusions presented above.

In summary, a series of four adducts of rhodium trifluoroacetate dimer with nitroxyl free radicals have been prepared, and their structural and magnetic properties studied. Different nitroxyl–metal geometries and magnetic behaviors have been observed. Local symmetry considerations as well as extended Hückel calculations allow one to propose that the intramolecular internitroxyl coupling is mediated by the Rh–Rh bond and involves mainly a σ mechanism.

Registry No. **1**·C_6H_6, 119679-72-0; **2**, 111468-86-1; **3**, 111468-87-2; **4**, 111468-89-4; $Rh_2(tfac)_4$, 31126-95-1; Rh, 7440-16-6.

Supplementary Material Available: Tables of crystal data summary (Table SI), bond lengths and angles (Tables SII–IX), and anisotropic thermal parameters (Tables SX–XIII) (16 pages); tables of observed and calculated structure factors (Tables SXIV–XVIII) (62 pages). Ordering information is given on any current masthead page.

Kinetics and Mechanism of Phosphine Substitution for CO in $[Fe_2Co(CO)_9(CCO)]^-$

Stanton Ching and Duward F. Shriver*

Contribution from the Department of Chemistry, Northwestern University, Evanston, Illinois 60208. *Received September 12, 1988*

Abstract: Rate laws and activation parameters were determined for CO substitution of $[PPN][Fe_2Co(CO)_9(CCO)]$ by phosphine ligands. These results along with the dependence of the reaction on the nature of the incoming ligand support an associative mechanism. Previous NMR data indicate that the phosphines selectively attack the Co metal center. Activation parameters are $\Delta H^\ddagger = +7.2$ to $+10.3$ kcal/mol and $\Delta S^\ddagger = -34.0$ to -45.5 cal/mol K. The activated complex is proposed to attain an open structure by breaking either a metal–metal or metal–carbon bond. An increase in solvent polarity increases the rate of ligand substitution, whereas a change in the cation from PPN^+ to Me_4N^+ has a negligible effect. The rates of reaction were influenced by both the basicity and steric properties of the phosphines.

The reactions of molecular metal clusters present a mechanistic challenge because they are potentially more complex than reactions at single metal centers. An ensemble of metal atoms may undergo structural changes through modifications in both metal–metal and metal–ligand bonding.[1] Consequently, reactive sites and transition states can be difficult to determine. Metal–metal bonds are typically weak in comparison to metal–ligand bonds,[2] so cluster

(1) (a) Band, E.; Muetterties, E. L. *Chem. Rev.* **1978**, *78*, 639. (b) Evans, J. *Adv. Organomet. Chem.* **1977**, *16*, 319.

0002-7863/89/1511-3238$01.50/0

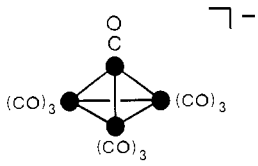

Figure 1. $[Fe_2Co(CO)_9(CCO)]^-$ represented as $[M_4(CO)_{10}]^-$.

fragmentation must also be considered. Mechanistic studies of ligand transformations on metal clusters contribute to the fundamental understanding of how metal ensembles influence ligand bonding and reactivity. This information may provide clues for reaction mechanisms on metal surfaces and homogeneous catalysis by clusters.[3]

Mechanistic studies of low-valent metal clusters have primarily focused on CO substitution reactions, and the most detailed kinetic investigations to date have been performed on simple binary carbonyl clusters.[4] Studies on each member of the $M_3(CO)_{12}$ series (M = Fe, Ru, and Os) have been reported,[5-8] and the kinetic behavior of the tetranuclear systems $Co_4(CO)_{12}$[9] and $Ir_4(CO)_{12}$[10] and their derivatives[11,12] has been examined in great detail. Kinetic measurements of ligand substitution rates are also known for mixed-metal[13-15] and heteroatom-capped carbonyl clusters,[15,16] but these are less common. Mixed-metal clusters are especially interesting systems to study because they offer the possibility of reaction pathways that are site-selective and mechanisms that can involve cooperative interactions between a substrate and different metal atoms.[17]

The anionic, mixed-metal cluster $[Fe_2Co(CO)_9(\mu_3\text{-}CCO)]^-$ can be viewed by isolobal analogy[18] and other theoretical treatments of cluster bonding[19,20] as a heteroatomic, tetranuclear carbonyl cluster $[Fe_2CoC(CO)_{10}]^-$ (Figure 1). This analogy was initially suggested from the behavior of the cluster toward CO exchange. Under a ^{13}CO atmosphere, $[Fe_2Co(CO)_9(CCO)]^-$ becomes ^{13}C enriched at all 10 CO ligands on the cluster[21] (eq 1). Thus it appears that the carbon-bound carbonyl ligand undergoes CO exchange as though it was coordinated to a metal atom.

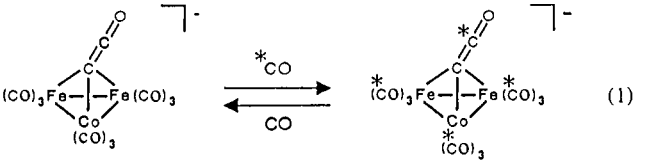

(1)

In this paper and the one following, we present a detailed kinetic investigation of the CO substitution chemistry of $[Fe_2Co(CO)_9(CCO)]^-$. The reaction is site-specific and occurs in two steps[22,23] (eq 2). The initial intermolecular substitution is discussed here.

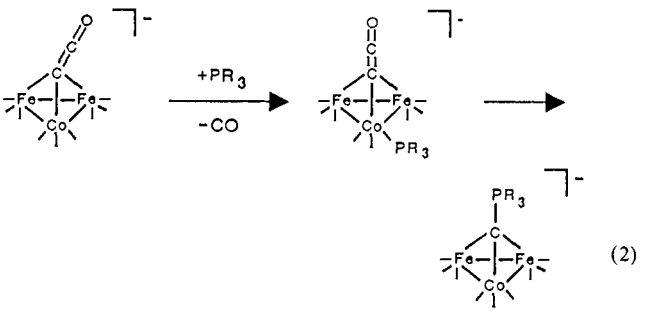

(2)

Experimental Section

General Procedures, Materials, and Instrumentation. All manipulations were carried out under a purified N_2 atmosphere with standard Schlenk and syringe techniques[24] or in a Vacuum Atmospheres drybox. Solvents were typically reagent grade and were distilled from appropriate drying agents and deaerated prior to use.[25] The ligands PMe_3, PMe_2Ph, $PMePh_2$, PEt_3, PEt_2Ph, $P(OMe)_3$, and $P(OPh)_3$ (Strem) were used as received and stored under a N_2 atmosphere unless impurity was detected by ^1H or ^{31}P NMR spectroscopy. Contaminated phosphines were purified by distillation from Na under reduced pressure. $[PPN][Fe_2Co(CO)_9(CCO)]$ was prepared by a published procedure[21] [PPN, bis(triphenylphosphine)nitrogen(1+)]. The clusters $[PPN][Fe_2Co(CO)_8L(CCO)]$ (L, ligands described above, excepting PEt_2Ph) have been previously characterized.[23]

Infrared spectra were recorded with a Nicolet 7199 FT-IR spectrometer using solution cells with CaF_2 windows and a 0.1-mm path length or a Specac 20.500 variable-temperature IR cell with AgCl windows and a 0.5-mm path length. Constant temperature was maintained with a Neslab RTE-8 external circulating bath (±0.1 °C). NMR spectra were recorded with a Varian XL-400 spectrometer (^1H, 399.942 MHz; ^{13}C, 100.577 MHz; ^{31}P, 161.905 MHz). NMR chemical shifts are reported with respect to standard references (^1H and ^{13}C, TMS; ^{31}P, 85% H_3PO_4) and deshielded resonances are taken as positive.

Characterization of $[PPN][Fe_2Co(CO)_8(PEt_2Ph)(CCO)]$. This cluster was spectroscopically characterized in solution without isolation: IR, ν_{CO} (CH_2Cl_2) 2037 (w), 1967 (s) cm^{-1}; ^1H NMR (CD_2Cl_2, + 25 °C) 7.8–7.3 (Ph, overlapping with PPN^+), 1.99 (m, CH_2), 1.17 (m, CH_3) ppm; ^{31}P NMR (CD_2Cl_2, −90 °C) 46.7 (br) ppm; ^{13}C NMR (CD_2Cl_2, −90 °C) 216.3 (CO), 180.7 (d on s, $^1J_{CC}$ = 72.5 Hz, CCO), 91.7 (br, CCO) ppm.

$[Me_4N][Fe_2Co(CO)_9(CCO)]$. A 2.30-g (1.50-mmol) sample of $[PPN]_2[Fe_3(CO)_9(CCO)]$[26] and 2.1 g (6.0 mmol) of $K[BPh_4]$ were stirred in 18 mL of THF for 2 h and filtered. The solvent was removed under

(2) Connor, J. A. *Top. Curr. Chem.* **1977**, *71*, 71.
(3) (a) Parshall, G. W. *Homogeneous Catalysis*; Wiley: New York, 1980. (b) Kochi, J. K. *Organometallic Mechanisms and Catalysis*; Academic: New York, 1978.
(4) Poë, A. J. In *Metal Clusters*; Moskowitz, M., Ed.; Wiley-Interscience: New York, 1986; Chapter 4.
(5) (a) Kumar, R. *J. Organomet. Chem.* **1977**, *136*, 235. (b) Shojaie, A.; Atwood, J. D. *Organometallics* **1985**, *4*, 187.
(6) (a) Candlin, J. P.; Shortland, A. C. *J. Organomet. Chem.* **1969**, *16*, 289. (b) Poë, A.; Twigg, M. V. *J. Chem. Soc., Dalton Trans.* **1974**, 1860. (c) Poë, A.; Twigg, M. V. *Inorg. Chem.* **1974**, *13*, 2982. (d) Twigg, M. V. *Inorg. Chim. Acta* **1977**, *21*, L7. (e) Ambwani, B.; Chawla, S.; Poë, A. *Inorg. Chem.* **1985**, *24*, 2635. (f) Ambwani, B.; Chawla, S.; Poë, A. J. *Inorg. Chim. Acta* **1987**, *133*, 93.
(7) (a) Poë, A.; Sekhar, V. C. *Inorg. Chem.* **1985**, *24*, 4376. (b) Brodie, N.; Poë, A.; Sekhar, V. *J. Chem. Soc., Chem. Commun.* **1985**, 1090. (c) Poë, A. J.; Sampson, C. N.; Smith, R. T. *J. Am. Chem. Soc.* **1986**, *108*, 5459.
(8) Shen, J.-K.; Shi, Y.-L.; Gao, Y.-C.; Shi, Q.-Z.; Basolo, F. *J. Am. Chem. Soc.* **1988**, *110*, 2414.
(9) (a) Darensbourg, D. J.; Incorvia, M. J. *Inorg. Chem.* **1980**, *19*, 2585. (b) Huq, R.; Poë, A. *J. Organomet. Chem.* **1982**, *226*, 277.
(10) (a) Karel, K. J.; Norton, J. R. *J. Am. Chem. Soc.* **1974**, *96*, 6812. (b) Sonnenberger, D.; Atwood, J. D. *Inorg. Chem.* **1981**, *20*, 3243. (c) Stuntz, G. F.; Shapley, J. R. *J. Organomet. Chem.* **1981**, *213*, 389.
(11) (a) Darensbourg, D. J.; Incorvia, M. J. *J. Organomet. Chem.* **1979**, *171*, 89. (b) Darensbourg, D. J.; Zalewski, D. J. *Organometallics* **1985**, *4*, 92.
(12) (a) Darensbourg, D. J.; Baldwin-Zuschke, B. J. *Inorg. Chem.* **1981**, *20*, 3846. (b) Sonnenberger, D. C.; Atwood, J. D. *J. Am. Chem. Soc.* **1982**, *104*, 2113. (c) Darensbourg, D. J.; Baldwin-Zuschke, B. J. *J. Am. Chem. Soc.* **1982**, *104*, 3906. (d) Sonnenberger, D. C.; Atwood, J. D. *Organometallics* **1982**, *1*, 694.
(13) (a) Fox, J. R.; Gladfelter, W. L.; Geoffroy, G. L. *Inorg. Chem.* **1980**, *19*, 2574. (b) Fox, J. R.; Gladfelter, W. L.; Wood, T. G.; Smegal, J. A.; Foreman, T. K.; Geoffroy, G. .; Tavanaiepour, I.; Day, V. W.; Day, C. S. *Inorg. Chem.* **1981**, *20*, 3214.
(14) (a) Shojaie, R.; Atwood, J. D. *Inorg. Chem.* **1987**, *26*, 2199. (b) Shojaie, R.; Atwood, J. D. *Inorg. Chem.* **1988**, *27*, 2558.
(15) Rossetti, R.; Gervasio, G.; Stanghelini, P. L. *J. Chem. Soc., Dalton Trans.* **1978**, 222.
(16) (a) Cetini, G.; Stanghellini, P. L.; Rossetti, R.; Gambino, O. *Inorg. Chim. Acta* **1968**, *2*, 433. (b) Rossetti, R.; Stanghellini, P. L.; Gambino, O.; Cetini, G. *Inorg. Chim. Acta* **1972**, *6*, 205.
(17) Gladfelter, W. L.; Geoffroy, G. L. *Adv. Organomet. Chem.* **1980**, *18*, 207.
(18) Hoffmann, R. *Angew. Chem., Int. Ed. Engl.* **1982**, *21*, 711.
(19) Wade, K. *Adv. Inorg. Chem. Radiochem.* **1976**, *18*, 1.
(20) Mingos, D. M. P. *Acc. Chem. Res.* **1984**, *19*, 311.
(21) Ching, S.; Holt, E. M.; Kolis, J. W.; Shriver, D. F. *Organometallics* **1988**, *7*, 892.
(22) Ching, S.; Sabat, M.; Shriver, D. F. *J. Am. Chem. Soc.* **1987**, *109*, 4722.
(23) Ching, S.; Sabat, M.; Shriver, D. F. *Organometallics*, in press.
(24) Shriver, D. F.; Drezdzon, M. A. *The Manipulation of Air-Sensitive Compounds*, 2nd ed.; Wiley: New York, 1986.
(25) Gordon, A. J.; Ford, R. A. *The Chemists' Companion*; Wiley: New York, 1972.
(26) Hriljac, J. A.; Shriver, D. F. *J. Am. Chem. Soc.* **1987**, *109*, 6010.

Table I. Infrared ν_{CO} Data for [PPN][$Fe_2Co(CO)_9(CCO)$] (**1**) and [PPN][$Fe_2Co(CO)_8(PR_3)(CCO)$] (**2a–g**) in CH_2Cl_2

Compd	ν_{CO}, cm^{-1}	Compd	ν_{CO}, cm^{-1}
1	2068 (w), 1999 (s), 1928 (m)	**2d**	2035 (w), 1965 (s)
2a	2037 (w), 1964 (s)	**2e**	2037 (w), 1967 (s)
2b	2037 (w), 1966 (s)	**2f**	2046 (w), 1977 (s)
2c	2039 (w), 1968 (s)	**2g**	2049 (w), 1980 (s)

vacuum and 15 mL of Et_2O was added followed by 20 mL of THF. The solution of $K_2Fe_3(CO)_9(CCO)$ was filtered (removing excess K[BPh_4] and [PPN][BPh_4]) onto 0.50 g (4.5 mmol) of [Me_4N]Cl, which gave a red precipitate. The liquids were removed under vacuum, and the solid was dissolved in 5 mL of acetone. The solution was filtered (removing [Me_4N]Cl and KCl), and 20 mL of Et_2O was added to produce [Me_4N]$_2$[$Fe_3(CO)_9(CCO)$] as a red solid which was isolated by filtration and vacuum dried; 0.80 g isolated. A 0.70-g (1.2-mmol) sample of this product was reacted with a 0.47 g (1.4 mmol) of $Co_2(CO)_8$ in 10 mL of THF under a CO atmosphere for 10 min. The solvent was removed under vacuum and 8 mL of CH_2Cl_2 was added followed by 2 mL of MeI. Some black solids and colorless [Me_4N]I crystals precipitated, and after 10 min the solution was filtered. Pentane (20 mL) was added to precipitate [Me_4N][$Fe_2Co(CO)_9(CCO)$] as a black powder which was isolated by filtration and vacuum dried; yield, 0.14 g (23% from [Me_4N]$_2$[$Fe_3(CO)_9(CCO)$]). Integration of the ^1H NMR resonances indicated 90% conversion to the Me_4N^+ salt and 10% as the PPN^+ salt: IR ν_{CO} (CH_2Cl_2) 2068 (w), 2001 (s), 1931 (m) cm^{-1}, in agreement with the IR spectrum of [PPN][$Fe_2Co(CO)_9(CCO)$].[21]

Kinetic Measurements. Unless otherwise noted, reactions were performed under pseudo-first-order conditions with the ligand in 40-fold molar excess or greater relative to the cluster. In a typical experiment, a septum-capped Schlenk flask containing a CH_2Cl_2 solution of the cluster (5.0×10^{-3} M) was treated with a measured amount of ligand. An aliquot of the reaction mixture was then transferred by syringe into a solution IR cell, which had been flushed with N_2 and capped with septa. For reactions of less than 15 min at room temperature, no temperature regulation was employed. All other reactions were maintained at constant temperature with an external circulating bath.

Rate data were obtained by monitoring the disappearance of a weak but well-resolved IR band at 2068 cm^{-1} characteristic of the starting material. Plots of $-\ln A$ vs time were linear over a period of 2–3 half-lives (linear correlation coefficient, >0.999) and the slopes of these lines yielded k_{obsd}. Measurement of IR bands due to the appearance of products (2050–2035 cm^{-1}) gave similar rate constants for those reactions in which the subsequent migration was slow.[22,23] Values of k_2 were obtained from plots of k_{obsd} vs ligand concentration for room temperature data and from k_{obsd}/(ligand concentration) for variable-temperature measurements. Eyring plots of rates measured over a 20–30 °C temperature range gave ΔH^* and ΔS^*. The rates of reaction were found to be insensitive to light and tolerant of brief exposures to air.

Results and Discussion

Rate Behavior and Mechanism. Phosphine substitution of [PPN][$Fe_2Co(CO)_9(CCO)$] (**1**) is sufficiently rapid so that rates in CH_2Cl_2 can be measured without interference from subsequent ligand migration (eq 2). The reaction is general[23] for phosphine ligands with relatively small cone angles[27] (eq 3). Bulky ligands

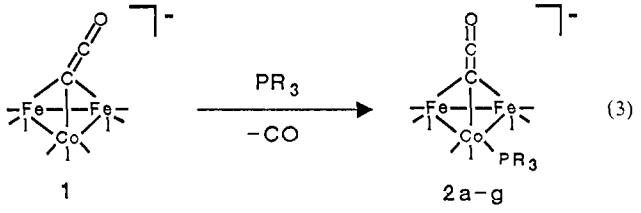

(3)

PR_3 = PMe_3 (a), PMe_2Ph (b), $PMePh_2$ (c), PEt_3 (d), PEt_2Ph (e), $P(OMe)_3$ (f), $P(OPh)_3$ (g)

such as PPh_3 and $P(C_6H_{11})_3$ do not react with **1**. Reactions were monitored by following changes in the infrared absorbance spectra with time. Spectral changes in the ν_{CO} region exhibit clean isosbestic points for reactions that are completed prior to the onset of phosphine migration (Figure 2). However, under conditions in which migration occurs before ligand substitution is complete, slightly uneven isosbestic points are observed (Figure 3). Infrared

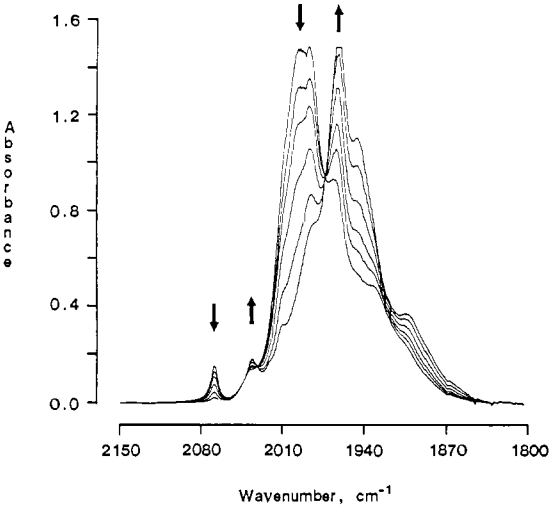

Figure 2. Time-dependent IR spectra recorded in the ν_{CO} region of the reaction [PPN][$Fe_2Co(CO)_9(CCO)$] + PEt_3 → [PPN][$Fe_2Co(CO)_8(PEt_3)(CCO)$] + CO in CH_2Cl_2 at room temperature.

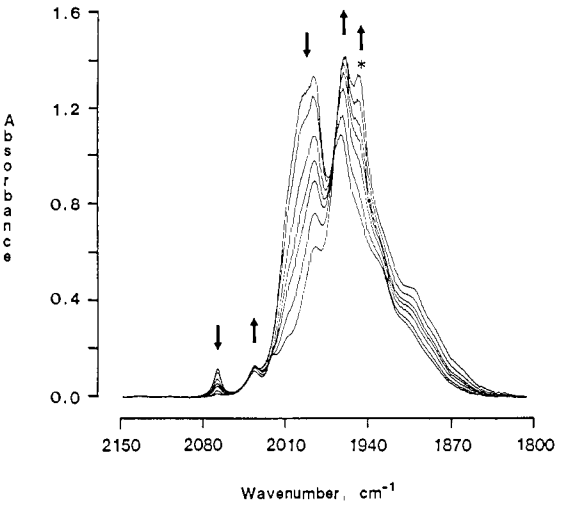

Figure 3. Time-dependent IR spectra recorded in the ν_{CO} region for the reaction [PPN][$Fe_2Co(CO)_9(CCO)$] + PMe_3 → [PPN][$Fe_2Co(CO)_8(PMe_3)(CCO)$] + CO in CH_2Cl_2 at room temperature. The absorbance band marked with an asterisk is due to the formation of [PPN][$Fe_2Co(CO)_9(CPMe_3)$].[22]

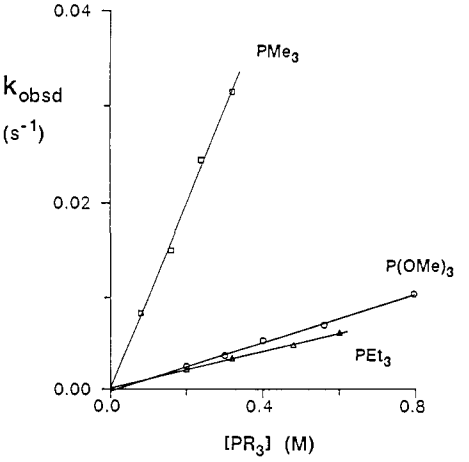

Figure 4. Plots of k_{obsd} vs phosphine concentration for CO substitution of [PPN][$Fe_2Co(CO)_9(CCO)$] by PR_3 in CH_2Cl_2 at room temperature. PR_3 = PMe_3, $P(OMe)_3$, and PEt_3.

(27) Tolman, C. A. *Chem. Rev.* **1977**, *77*, 313.

Table II. Second-Order Rate Constants and Activation Parameters for CO Substitution Reactions of $[PPN][Fe_2Co(CO)_9(CCO)]$ in CH_2Cl_2[a]

compd	L	T, °C	k_2, M^{-1} s^{-1} [b]	$\Delta H^{\ddagger}$, kcal mol^{-1}	$\Delta S^{\ddagger}$, cal mol^{-1} K^{-1}
2a	PMe_3	3.0	3.92 (3) × 10^{-2}	+8.5 (2)	−34.0 (7)
		9.0	5.86 (5) × 10^{-2}		
		15.1	7.78 (6) × 10^{-2}		
		23.3	1.22 (1) × 10^{-1}		
		29.3	1.69 (1) × 10^{-1}		
2b	PMe_2Ph	3.0	2.99 (2) × 10^{-3}	+9.6 (1)	−35.2 (4)
		9.2	4.35 (2) × 10^{-3}		
		15.0	6.28 (3) × 10^{-3}		
		23.7	1.08 (1) × 10^{-2}		
		29.4	1.49 (2) × 10^{-2}		
2c	$PMePh_2$	14.7	2.492 (5) × 10^{-4}	+10.3 (4)	−39 (1)
		21.5	4.05 (1) × 10^{-4}		
		27.5	5.83 (2) × 10^{-4}		
		33.1	7.84 (1) × 10^{-4}		
2d	PEt_3	3.1	3.468 (6) × 10^{-3}	+7.2 (3)	−43.6 (9)
		9.4	4.972 (8) × 10^{-3}		
		15.0	6.14 (2) × 10^{-3}		
		23.7	9.67 (6) × 10^{-3}		
		29.7	1.196 (5) × 10^{-2}		
2e	PEt_2Ph	15.8	6.7 (1) × 10^{-4}	+9.0 (3)	−42 (1)
		23.3	9.99 (3) × 10^{-4}		
		30.6	1.440 (4) × 10^{-3}		
		38.0	2.22 (1) × 10^{-3}		
2f	$P(OMe)_3$	−1.6	3.02 (2) × 10^{-3}	+7.6 (1)	−42.0 (5)
		9.0	5.65 (3) × 10^{-3}		
		14.5	7.66 (1) × 10^{-3}		
		25.3	1.192 (7) × 10^{-2}		
		30.8	1.54 (2) × 10^{-2}		
2g	$P(OPh)_3$	13.2	9.6 (1) × 10^{-5}	+8.8 (1)	−45.5 (2)
		21.1	1.48 (3) × 10^{-4}		
		29.1	2.3 (1) × 10^{-4}		
		34.6	3.0 (1) × 10^{-4}		

[a] Equation 3. [b] Errors reported are standard deviations.

bands of **1** and substituted clusters **2a–g** are listed in Table I. The phosphine ligands are not displaced by CO at 1 atm and cluster fragmentation is not evident in any of the reactions.

Kinetic data for CO substitution of **1** strongly support an associative mechanism. The rates of reaction are highly dependent on both the nature and concentration of the phosphine ligand. Sample plots of k_{obsd} versus $[PR_3]$ are given in Figure 4. In all cases, y intercepts are within experimental error of the origin and first-order behavior is observed with respect to phosphine concentration. Thus, the reactions of **1** with phosphines obey the overall second-order rate law given by eq 4. Activation param-

$$-d[\mathbf{1}]/dt = k_2[\mathbf{1}][PR_3] \quad (4)$$

eters, $\Delta H^{\ddagger}$ and $\Delta S^{\ddagger}$, are given in Table II. The relatively small values of $\Delta H^{\ddagger}$ and large, negative values of $\Delta S^{\ddagger}$ indicate that bond making is important in the formation of the activated complex. An associative mechanism is also consistent with the qualitative observation that bulky phosphines do not react with **1**. Previous kinetic studies on CO substitution of mixed-metal dinuclear[28] and cluster[15,29] compounds containing Fe and Co metal centers also indicate associative mechanisms.

Variable-temperature ^{13}C and ^{31}P NMR spectroscopy establishes that the phosphine ligands bind selectively to the Co atom in **1**.[23] The reason for substitution at the Co atom rather than one of the Fe centers is not clear, but this phenomenon is well-known for other compounds containing both Fe and Co atoms.[15,28-30] Cobalt metal sites are also more substitutionally labile in homometallic carbonyl compounds. For example, ligand substitution of $Co_2(CO)_8$[31] and $Co_4(CO)_{12}$[9] occurs rapidly in comparison to that of $Fe(CO)_5$[31,32] and $Fe_3(CO)_{12}$.[5]

Scheme I

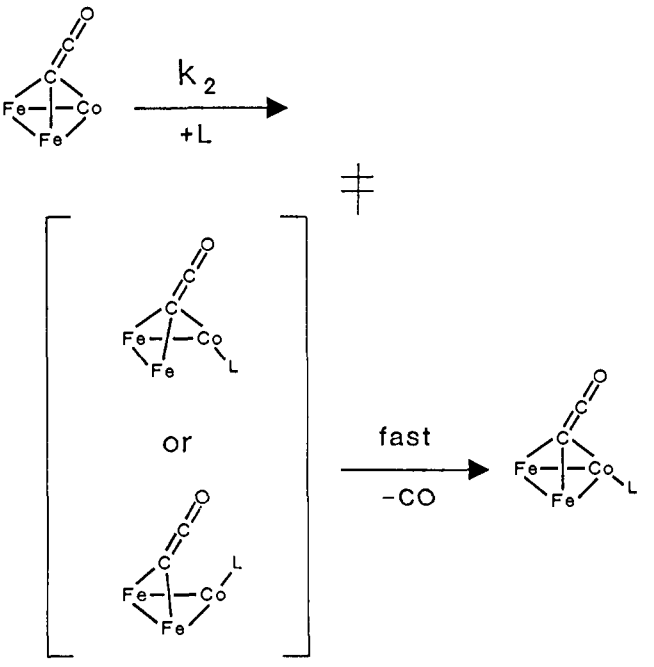

Possible mechanisms for CO substitution of **1** are proposed in Schemes I and II. Initial metal–metal bond scission is commonly invoked in associative reactions of metal clusters.[33] This structural change allows the cluster to accept the additional pair of valence electrons from an entering nucleophile (Scheme I). In addition, a cluster such as **1** may develop an open coordination site by cleavage of a metal–carbon bond with the formation of a μ_2-CCO. Changes in coordination from μ_3 to μ_2 have been observed for nucleophilic attack on clusters with capping thiolate[34] and iodide[35] ligands. A similar mechanism can also be proposed for associative ligand substitution on chalcogen-capped carbonyl clusters.[15,16] A test to distinguish metal–metal from metal–carbon cleavage has not been devised.

An alternate to the mechanisms in Scheme I is a dissociative preequilibrium involving **1** and some unsaturated intermediate that subsequently adds a phosphine ligand (Scheme II). Such a mechanism is indistinguishable from Scheme I based solely on the form of the rate law given in eq 4. The rate expression for the preequilibrium mechanism is shown in eq 5. At sufficiently

$$\frac{-d[\mathbf{1}]}{dt} = \frac{k_1k_2[\mathbf{1}][PR_3]}{k_{-1} + k_2[PR_3]} \quad (5)$$

high concentrations of phosphine ligand, the system saturates and the expression becomes independent of ligand concentration provided that $k_2[PR_3] \gg k_{-1}$. However, saturation is not observed for the reaction of **1** with PMe_3 up to a ligand concentration of 0.321 M. Beyond this concentration the rate becomes too fast to measure by conventional IR methods. Although these results disfavor a preequilibrium mechanism, they do not eliminate it as a possibility since the concentration of PMe_3 may be too low or the magnitudes of k_{-1} and k_2 in eq 5 may be insufficient to observe saturation. In principle, steric bulk of the incoming ligand might differentiate direct phosphine attack in Scheme I from the mechanism with cluster-opening preequilibrium, Scheme II. This issue will be discussed below.

Solvent and Cation Effects. Kinetics of CO substitution of $[PPN][Fe_2Co(CO)_9(CCO)]$ by PEt_3 were measured in different solvents under identical conditions of concentration and tem-

(28) Jackson, R. A.; Kanluen, R.; Poë, A. *Inorg. Chem.* **1981**, *20*, 1130.
(29) Planalp, R. P.; Vahrenkamp, H. *Organometallics* **1987**, *6*, 492.
(30) (a) Cooke, C. G.; Mays, M. J. *J. Organomet. Chem.* **1974**, *74*, 449. (b) Huie, B. T.; Knobler, C. B.; Kaesz, H. D. *J. Am. Chem. Soc.* **1978**, *100*, 3059. (c) Aime, S.; Milone, L.; Rossetti, R.; Stanghellini, P. L. *Inorg. Chim. Acta* **1977**, *25*, 103. (d) Langenbach, H.-J.; Vahrenkamp, H. *Chem. Ber.* **1979**, *112*, 3390. (e) Low, A. A.; Lauher, J. W. *Inorg. Chem.* **1987**, *26*, 3863. (f) Albiez, T.; Vahrenkamp, H. *Angew. Chem., Int. Ed. Engl.* **1987**, *26*, 572.
(31) Manuel, T. A. *Adv. Organomet. Chem.* **1965**, *3*, 181, and references therein.
(32) Siefert, E. E.; Angelici, R. J. *J. Organomet. Chem.* **1967**, *8*, 374.
(33) Vahrenkamp, H. *Adv. Organomet. Chem.* **1983**, *22*, 169.
(34) Johnson, B. F. G.; Lewis, J.; Pippard, D. A. *J. Organomet. Chem.* **1981**, *213*, 249.
(35) Johnson, B. F. G.; Lewis, J.; Pippard, D. A. *J. Chem. Soc., Dalton Trans.* **1981**, *407*.

Scheme II

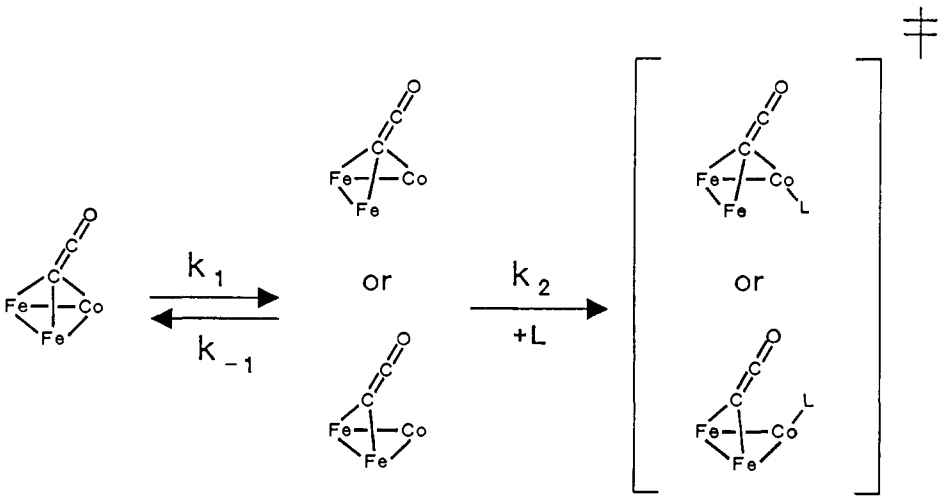

Table III. Second-Order Rate Constants for the Reaction $[Fe_2Co(CO)_9(CCO)]^- + PEt_3 \rightarrow [Fe_2Co(CO)_8(PEt_3)(CCO)]^- + CO$

cation	solvent	k_2, M^{-1} s^{-1} [a]	k_2(rel)	ϵ	E_T [b]	DN [c]
PPN^+ [d]	THF	2.69 (3) × 10^{-3}	1	7.4	37.4	20.0
	CH_2Cl_2	1.12 (1) × 10^{-2}	4	8.9	41.1	
	acetone	1.61 (1) × 10^{-2}	6	17.0	42.2	17.0
	MeCN	8.31 (9) × 10^{-2}	31	14.1	46.0	14.1
Me_4N^+ [e]	THF	5.40 (5) × 10^{-3}	1	7.4	37.4	20.0
	CH_2Cl_2	2.51 (2) × 10^{-2}	5	8.9	41.1	
	acetone	1.44 (1) × 10^{-2}	3	17.0	42.2	17.0
	MeCN	1.04 (1) × 10^{-1}	19	14.1	46.0	14.1

[a] Errors reported are standard deviations. [b] Empirical parameters for solvent polarity derived from the solvatochromic behavior of pyridinium *N*-phenolbetaine.[36] [c] DN = $-\Delta H$(EPD·$SbCl_5$) for the reaction EPD + $SbCl_5 \rightarrow$ EPD·$SbCl_5$ in 1,2-dichloroethane, in which EPD is an electron pair donor.[37] [d] Rates measured at 27.2 °C. [e] Rates measured at 26.0 °C and corrected for 9:1 Me_4N^+/PPN^+.

perature. Correlations were sought between the rate constants and solvent dielectric constants (ϵ), empirical polarity parameters (E_T),[36] and donor numbers (DN)[37] (Table III). Rate constants increase with solvent polarity, as indicated by ϵ and E_T. This finding suggests that ligand substitution on $[Fe_2Co(CO)_9(CCO)]^-$ proceeds through a transition state that is more polar than the ground state. Substantial polarization of the transition state is not expected since neither the entering nucleophile (PR_3) nor the leaving group (CO) is charged. Indeed, rates of reaction for this negatively charged cluster are not as solvent dependent as rates of reaction that involve charge-separated transition states. There is no relationship with donor number (DN), so it is doubtful that solvent coordination plays a significant role in the rate-determining step.

Changing the cation of $[Fe_2Co(CO)_9(CCO)]^-$ from PPN^+ to Me_4N^+ does not produce large changes in substitution rates in any of the solvents studied. Thus, the influence of solvent on cation–anion interactions is believed to be negligible with large cations such as PPN^+ and Me_4N^+. There are relatively few kinetic studies of substitution reactions on charged clusters[38-40] and the effects of solvents and counterions on these reactions are not well-known.

Steric and Electronic Profiles. Second-order rate constants for the reaction of **1** with various phosphine ligands at 25 °C are listed in Table IV and a plot of log k_2 versus ΔHNP of the ligands is shown in Figure 5. The values of ΔHNP represent the differences in the half neutralization potentials for the free phosphine ligands in nitromethane solution with *N,N'*-diphenylguanidine taken as the standard.[41] Linear free energy relationships can be derived from plots of log k_2 versus ΔHNP,[42] but good correlations rely on the absence of significant steric effects. A poor correlation is observed in Figure 5, which suggests that steric factors play an important role in CO substitution of **1**. This proposal is supported by a large discrepancy in the rates of reaction for PMe_3 and PEt_3 in spite of their similar basicities. The influence of ligand size on reactivity is also evident from the lack of reactivity between **1** and the very basic, but bulky $P(C_6H_{11})_3$. Such steric influences might be expected for cluster compounds given the crowded ligand environment. The pathway involving direct phosphine attack (Scheme I) should be more sensitive to steric factors than the alternative cluster opening preequilibrium (Scheme II). The

Table IV. Second-Order Rate Constants for CO Substitution Reactions of $[PPN][Fe_2Co(CO)_9(CCO)]$ at 25 °C in CH_2Cl_2 with Electronic and Steric Parameters

compd	L	k_2, M^{-1} s^{-1} [a]	log k_2	ΔHNP [b]	θ [c]	Δlog k_2
2a	PMe_3	1.34 × 10^{-1}	−0.87	114	118	1.52
2b	PMe_2Ph	1.14 × 10^{-2}	−1.94	281	122	0.96
2c	$PMePh_2$	4.56 × 10^{-4}	−3.34	424	136	0.00
2d	PEt_3	9.90 × 10^{-3}	−2.00	111	132	0.38
2e	PEt_2Ph	1.09 × 10^{-3}	−2.96	300	136	0.00
2f	$P(OMe)_3$	1.19 × 10^{-2}	−1.92	580 [d]	107	1.90
2g	$P(OPh)_3$	2.39 × 10^{-4}	−3.62	875	128	1.10

[a] Rate constants for 25 °C are obtained from Eyring plots of the data in Table II. [b] Values taken from ref 41–43. [c] Reference 27. [d] Estimated value.

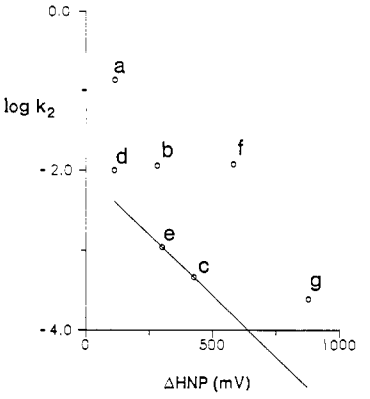

Figure 5. Electronic profile for CO substitution of $[PPN][Fe_2Co(CO)_9(CCO)]$ in CH_2Cl_2. Points represent rate data for 25 °C. Lettering scheme is given in Table IV.

(36) Reichardt, C. *Angew. Chem., Int. Ed. Engl.* **1965**, *4*, 29.
(37) Mayer, U.; Gutmann, V. *Struct. Bonding (Berlin)* **1972**, *12*, 113.
(38) Anstock, M.; Taube, D.; Gross, D. C.; Ford, P. C. *J. Am. Chem. Soc.* **1984**, *106*, 3696.
(39) Taube, D. J.; Ford, P. C. *Organometallics* **1986**, *5*, 99.
(40) Housecroft, C. E.; Fehlner, T. P. *J. Am. Chem. Soc.* **1986**, *108*, 4867.
(41) Streuli, C. A. *Anal. Chem.* **1960**, *32*, 985.
(42) Thorsteinson, E. M.; Basolo, F. *J. Am. Chem. Soc.* **1966**, *88*, 3929.
(43) Chang, C.-Y.; Johnson, C. E.; Richmond, T. G.; Chen, Y.-T.; Trogler, W. C.; Basolo, F. *Inorg. Chem.* **1981**, *20*, 3167.

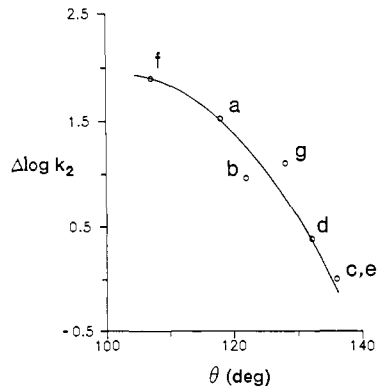

Figure 6. Steric profile for CO substitution of $[PPN][Fe_2Co(CO)_9(CCO)]$ in CH_2Cl_2. Points represent rate data for 25 °C. Lettering scheme is given in Table IV.

observed sensitivity to bulk of the incoming phosphine thus favors Scheme I, but it does not rule out Scheme II because the opening of the cluster may not relieve all of the steric crowding with the attacking ligand.

An empirical method of relating reaction rates to electronic and steric characteristics of the entering nucleophiles[44,45] has been applied to the data in Table IV. The electronic profile for ligand substitution of **1** is given by the plot of log k_2 versus ΔHNP (Figure 5), which correlates rates of reaction with phosphine basicities without considering steric factors. Points representing $PMePh_2$ and PEt_2Ph are joined, since these ligands have identical cone angles. Since size is held constant, the line that is generated should reflect only changes due to differences in basicity. The gradient of this line reflects the sensitivity of the reaction rate to changes in phosphine basicity. It is proposed that the gradient is also proportional to the degree of bond making in the transition state between the metal atom and the entering ligand.[46] The value of $-0.0031\ mV^{-1}$ obtained from Figure 5 is the same as that found for CO substitution of $Ir_4(CO)_{12}$[45] but is on the low end of the scale for reactions of mononuclear complexes.[44]

Deviations of the other points from the line in Figure 5 (Δ log k_2) are attributed to steric factors for these ligands. A plot of Δ log k_2 versus θ generates a steric profile relating the rate of reaction to the size of the ligand (Figure 6), and a good correlation is observed. A steric threshold, θ_{st}, is defined as the cone angle below which steric contributions to the reaction rate become constant. For values of $\theta < \theta_{st}$, Δ log k_2 levels off in the steric profile. On the basis of Figure 6, the reaction of **1** with phosphines is quite sensitive to the size of the incoming ligand. A steric threshold for this reaction is not clearly defined, but a maximum value of $\theta_{st} = 115°$ is estimated even though the actual value may be much lower. It has been proposed that a steep gradient in the electronic profile coupled with a small value of θ_{st} indicates a congested transition state with substantial metal–ligand bonding while the inverse suggests an open transition state with little metal–ligand bonding.[44] In comparison with other kinetic data,[44,45] the results obtained for ligand substitution of **1** are intermediate. Thus, electronic and steric factors exert comparable influences in this reaction.

Conclusions

A kinetic investigation of CO substitution of $[Fe_2Co(CO)_9(CCO)]^-$ supports an associative reaction pathway. Phosphines react selectively at the Co atom. Proposed mechanisms invoke open polyhedra in the transition state resulting from Co–Fe bond breaking or Co–C bond cleavage. Both mechanisms are in accordance with the analogy of $[Fe_2Co(CO)_9(CCO)]^-$ to tetrametal carbonyl clusters. The response of the reaction rate to changes in solvent polarity and cation indicates that the transition state is more polar than the ground state. Rates of reaction are sensitive to changes in both the basicity and size of the phosphine ligand.

Acknowledgment. This research is funded by the NSF Program for Inorganic and Organometallic Chemistry. S.C. thanks Professor Fred Basolo and his research group for the use of their equipment and especially Dr. David L. Kershner for helpful discussions.

Registry No. 1, 88657-64-1; **2a**, 119145-53-8; **2b**, 119693-88-8; **2c**, 119145-57-2; **2d**, 119693-90-2; **2e**, 119693-92-4; **2f**, 119145-61-8; **2g**, 119145-63-0; $[PPN]_2[Fe_3(CO)_9(CCO)]$, 87710-96-1; $K_2Fe_3(CO)_9(CCO)$, 119693-83-3; $[Me_4N]_2[Fe_3(CO)_9(CCO)]$, 119693-84-4; $[Me_4N][Fe_2Co(CO)_9(CCO)]$, 119693-86-6; PMe_3, 594-09-2; PMe_2Ph, 672-66-2; $PMePh_2$, 1486-28-8; PEt_3, 554-70-1; PEt_2Ph, 1605-53-4; $P(OMe)_3$, 121-45-9; $P(OPh)_3$, 101-02-0.

(44) Golovin, M. N.; Rahman, M. M.; Belmonte, J. E.; Giering, W. P. *Organometallics* **1985**, *4*, 1981.
(45) (a) Dahlinger, K.; Falcone, F.; Poë, A. J. *Inorg. Chem.* **1986**, *25*, 2654. (b) Brodie, N. M. J.; Chen, L.; Poë, A. J. *Int. J. Chem. Kinet.* **1988**, *20*, 467. (c) Poë, A. *J. Pure Appl. Chem.* **1988**, *60*, 1209.
(46) Jackson, R. A.; Kanluen, R.; Poë, A. *Inorg. Chem.* **1984**, *23*, 523.

A Mechanistic Investigation of Phosphine Migration and Substitution in $[Fe_2Co(CO)_8(PR_3)(CCO)]^-$

Stanton Ching and Duward F. Shriver*

Contribution from the Department of Chemistry, Northwestern University, Evanston, Illinois 60208. *Received September 12, 1988*

Abstract: The kinetics of phosphine migration from a metal to a carbon site in a trimetallic cluster have been investigated. The rate of ligand migration is significantly decreased by bulky phosphines and is relatively insensitive to changes in phosphine basicity. Bridging phosphine and carbonyl ligands are proposed for the transition state, and pairwise exchange of these ligands is favored. Activation parameters for $PR_3 = PEt_3$, PEt_2Ph, and $PMePh_2$ are $\Delta H^\ddagger = +16.8$ to $+17.3$ kcal/mol and $\Delta S^\ddagger = -17$ to -21 cal/mol K. Reactions of small phosphines $[P(OMe)_3$, PMe_3, and $PMe_2Ph]$ contain an additional term in the rate law due to phosphine substitution for CO in $[PPN][Fe_2Co(CO)_8(PR_3)(CCO)]$, which gives $[PPN][Fe_2Co(CO)_8(PR_3)(CPR_3)]$. This reaction is in competition with ligand migration. Competition experiments and the observed steric barrier to substitution lead to the proposal that two phosphine ligands initially coordinate to the Co metal center and this is followed by a rapid intramolecular migration of one phosphine to the capping carbon atom. In the course of these mechanistic studies $[PPN][Fe_2Co(CO)_8(PMe_3)(CPMe_3)]$ has been isolated and characterized.

Carbonyl ligand migrations on metal clusters have been studied in numerous systems.[1,2] Such processes are conveniently observed on the NMR time scale and may relate to ligand mobility on surfaces.[3] Migrations of other species such as organic and hydride

0002-7863/89/1511-3243$01.50/0